The Cryosphere
Discussions

Open Access

EGU

Marine ice sheet model performance depends on basal sliding physics and sub-shelf melting

Rupert Michael Gladstone[1,2,3], Roland Charles Warner[2], Benjamin Keith Galton-Fenzi[2,4], Olivier Gagliardini[5,6], Thomas Zwinger[7], and Ralf Greve[8]

[1]VAW, Eidgenössische Technische Hochschule Zürich, ETHZ, Switzerland
[2]Antarctic Climate and Ecosystems Cooperative Research Centre, University of Tasmania, Hobart, Australia
[3]Arctic Centre, University of Lapland, Rovaniemi, Finland
[4]Australian Antarctic Division, Kingston, Tasmania, Australia
[5]CNRS, LGGE, F-38041 Grenoble, France
[6]Univ. Grenoble Alpes, LGGE, F-38041 Grenoble, France
[7]CSC – IT Center for Science Ltd., Espoo, Finland
[8]Institute of Low Temperature Science, Hokkaido University, Japan

Correspondence to: Rupert Gladstone (RupertGladstone1972@gmail.com)

Abstract.

Computer models are necessary for understanding and predicting marine ice sheet behaviour. However, there is uncertainty over implementation of physical processes at the ice base, both for grounded and floating glacial ice. Here we implement several sliding relations in a marine ice sheet flowline model accounting for all stress components, and demonstrate that model
5   resolution requirements are strongly dependent on both the choice of basal sliding relation and the spatial distribution of ice shelf basal melting.

Sliding relations that reduce the magnitude of the step change in basal drag from grounded ice to floating ice (where basal drag is set to zero) show reduced dependence on resolution compared to a commonly used relation, in which basal drag is purely a power law function of basal ice velocity. Sliding relations in which basal drag goes smoothly to zero as the grounding
10   line is approached from inland (due to a physically motivated incorporation of effective pressure at the bed) provide further reduction to resolution dependence.

A similar issue is found with the imposition of basal melt under the floating part of the ice shelf: melt parameterisations that reduce the abruptness of change in basal melting from grounded ice (where basal melt is set to zero) to floating ice provide improved convergence with resolution compared to parameterisations in which high melt occurs adjacent to the grounding line.
15   Thus physical processes, such as sub-glacial outflow (which could cause high melt near the grounding line), would impact on capability to simulate marine ice sheets.

For any given marine ice sheet the basal physics, both grounded and floating, governs the feasibility of simulating the system. The combination of a physical dependency of basal drag on effective pressure and low ice shelf basal melt rates near the grounding line mean that some marine ice sheet systems can be reliably simulated at a coarser resolution than currently
20   thought necessary.

1 Introduction

Ice Sheet Models (ISMs) are increasingly being used in process studies, sensitivity studies and projections of Marine Ice Sheet (MIS) future behaviour (Joughin et al., 2010; Favier et al., 2014; Gong et al., 2014), and Model Intercomparison Projects (MIPs) to investigate the ice sheet response to ocean forced basal melting of ice shelves are currently in their design phase (Asay-Davis
5 et al., 2015).

Past ISM studies have shown poor convergence of grounding line behaviour with increasing resolution (Vieli and Payne, 2005). Practical solutions have been suggested, such as parameterising the flux of ice across the grounding line as a function of ice thickness (Schoof, 2007; Pollard and DeConto, 2009), parameterising the grounding line position at sub-grid resolution (Gladstone et al., 2010b; Seroussi et al., 2014), or implementing adaptive mesh refinement to provide very high ISM
10 resolution at and near the grounding line (Cornford et al., 2013; Durand et al., 2009). These solutions all have limitations, and the computational cost of running a sufficiently high resolution ISM to robustly represent grounding line motion remains high, evenwith adaptive refinement.

However, model-based MIS studies (e.g. Pattyn et al. (2012)) typically use a simple basal traction prescription, or "sliding relation" (Weertman, 1957; Fowler, 2010), which neglects the impact of effective pressure at the bed (or equivalently
15 "height above bouyancy") on basal shear stress. The inclusion of pressure dependency, which has been proposed over 30 years ago (Budd et al., 1984), may affect the resolution requirements for successful grounding line modelling (Leguy et al., 2014; Tsai et al., 2015).

Furthermore, the implications of imposing basal melting (note that in the current study "basal melting" refers always to melting under the ice shelf and not the grounded part of the MIS) on resolution requirements have not been explicitly investigated.
20 In the current study, We assess the impact of choosing between different SRs, and between different approaches to parameterising basal melting, on model resolution requirements in a Stokes flow ISM.

2 Methods

We use the ice dynamic model Elmer/Ice (Gagliardini et al., 2013). Stokes equations for a viscous fluid with non-linear rheology are solved using the finite element method over a two-dimensional flowline domain (one vertical and one horizontal dimension)
25 in which lateral drag is parameterised (Gagliardini et al., 2010) according to channel width, W, and a contact problem is solved to determine the evolving grounding line position (Favier et al., 2012).

The rheology follows Glen's law (Glen, 1952; Paterson, 1994) with viscosity calculated using a temperature dependent Arrhenius law (Gagliardini et al., 2013; Paterson, 1994). Temperature is held constant at -10 C for all simulations in the current study.
30 We implement alternative sliding laws (Section 2.1) and a basal melt parameterisation (Section 2.2) in Elmer/Ice.

The Cryosphere

Discussions

Open Access

EGU

2.1 Basal sliding

The starting point for the sliding laws used in the current study is motivated by early laboratory sliding experiments and Antarctic simulations (Budd et al., 1979, 1984), which suggests modifying the original Weertman sliding relation (Weertman, 1957) by incorporating a power-law dependence of the drag on effective pressure at the bed as follows:

5
$$\tau_b^p = -C u_b^m z_*^q, \tag{1}$$

where τ_b is basal shear stress, u_b is basal ice velocity, z_* is the height above buoyancy (related to effective pressure at the bed, N, by $N = \rho_i g z_*$), m, p and q are constant exponents, and C is a constant sliding coefficient.

In the current study we set $m = \frac{1}{3}$ and $p = q = 1$ for all simulations. These values for p and q are chosen for simplicity, and deviate We impose $z_* \geq 0$ when calculating τ_b.

10
Ideally z_* would be calculated using basal water pressure from a sub-glacial hydrology model. In the current study, we simply use hydrostatic balance based on sea level,

$$z_* = \begin{cases} H, & \text{if } b >= 0 \\ H + b\frac{\rho_o}{\rho_i} & \text{if } b < 0 \end{cases} \tag{2}$$

where H is local ice thickness, b is the bedrock elevation relative to sea level (positive upwards), ρ_o is the density of ocean water, and ρ_i is the density of ice. This is equivalent to assuming a sub-glacial hydrology system fully connected to the ocean.

15
The four sliding relations used in the current study are given by

$$\tau_b = -C u_b^{\frac{1}{3}}, \tag{3}$$
$$\tau_b = -C u_b^{\frac{1}{3}} z_*, \tag{4}$$
$$\tau_b = -C u_b^{\frac{1}{3}} \frac{z_*}{H}, \tag{5}$$
$$\tau_b = -C u_b^{\frac{1}{3}} (z_* + z_o), \tag{6}$$

20
where z_o is a thickness offset.

The first two sliding relations (given by equations 3 and 4, and henceforth referred to as SR1 and SR2 respectively) are specific cases of equation 1 and derive from previously published sliding laws. SR1 is widely used in model intercomparison studies, such as the Marine Ice Sheet Model Intercomparison Project (MISMIP, Pattyn et al. (2012)). SR2 implements a smooth transition of basal drag to zero as the grounding line is approached from landwards.

25
SR3 (equation 5) uses thickness scaling to give a law which captures the smooth fade to zero of basal drag approaching the grounding line of SR2, but which equates to the familiar SR1 for ice grounded above sea level, providing ice sheet profiles more directly comparable to SR1.

The aim of SR4 (equation 6) is to provide a step-change in basal drag from grounded to floating ice, but one with significantly smaller magnitude than would occur with a Weertman-type (SR1) sliding relation.

30
The sliding relations and their coefficient values are summarised in Table 1.

The Cryosphere
Discussions

Open Access

EGU

2.2 Ice shelf basal melt

The ice shelf basal melt rate, m_b (calculated in m a^{-1} ice equivalent), is parameterised as a function of depth by

$$m_b = S_w S_i \frac{c_w \gamma_T}{L} \Omega \Delta T, \tag{7}$$

where ΔT is the "thermal driving", L is the latent heat of fusion, c_w is the heat capacity of seawater, γ_T is a heat transfer
5 coefficient, Ω is a dimensionless tuning parameter, and S_w and S_i are scaling factors.

The thermal driving is the far field to local temperature difference, $\Delta T = T_f - T_o$, where T_f is the local freezing point of
sea water, and T_o is the far field ocean temperature. T_f is approximated here in Centigrade using $T_f = -1.85 + 7.61 \times 10^{-4} z_i$,
where z_i is the depth of the ice base relative to sea level (positive upwards). We set $T_o = 2.0$ C.

This parameterisation is similar to that used in the "Marine Ice Sheet Ocean Model Intercomparison Project" phase 1 (MIS-
10 OMIP1), and is described in the MISOMIP1 experimental setup (Asay-Davis et al., 2015).

S_w is a scaling parameter used to reduce m_b smoothly to zero as the grounding line is approached from the ice shelf. It is
implemented as a function of water column thickness, H_w (given by $H_w = z_i - b$),

$$S_w = \tanh\left(e \frac{H_w}{H_{w0}}\right), \tag{8}$$

where H_{w0} is a reference water column thickness. S approaches 1 in deeper water ($H_w > H_{w0}$).
15 We present simulations both with and without the water column thickness scaling. Where it is used we set $H_{w0} = 100$m.
Where it is not used we set $S_w = 1$.

Iceberg calving is not represented in the current study, and the ice shelf front position remains fixed. This results in a
vanishingly thin ice shelf in some simulations and can cause numerical instabilities and model failures. S_i is an ice shelf depth
scaling parameter introduced to avoid the occurrence of a vanishingly thin ice shelf. S_i is given by

20 $$S_i = \max\left[\tanh\left(e \frac{z_{i0} - z_i}{z_s}\right), 0\right], \tag{9}$$

where z_{i0} is a reference ice base height relative to sea level (positive upwards) and z_s is a (directionless) scaling depth. In
practice the use of S_i gives zero melting for $z_i > z_{i0}$. The S_i scaling is used in all simulations with values $z_{i0} = -40$ m and
$z_s = 100$ m.

In the simulations presented here melt is applied to all mesh nodes in the floating part of the ice sheet. Simulations were also
25 carried out in which melting was also applied to the last grounded node, and this was found not to cause a large difference: the
results and interpretation presented here hold for both cases. The experiments are described in Section 2.3 and Table 3.

2.3 Experiment design

The experimental set up involves an 1800km domain with linear down sloping bedrock, b, given in km relative to sea level by

$$b = 0.2 - \frac{0.9x}{1800}, \tag{10}$$

where x is horizontal distance in km from the ice divide. This gives a bed rock elevation varying between $z = 200$ m and $z = -700$ m, where z is the vertical coordinate measured relative to sea level.

Net surface accumulation, a, is given in m a^{-1} by

$$a = \frac{x}{1800} \frac{\rho_o}{\rho_i}. \tag{11}$$

5   The upstream boundary represents the ice divide, and a Dirichlet condition is used here to set the horizontal component of velocity to zero, ensuring flow symmetry. An external hydrostatic pressure distribution imposed by the ocean (below sea level) is prescribed at the spatially fixed downstream calving front. This external pressure is also applied to the base of the ice shelf.

The mesh is composed of quadrilateral elements with 11 equally spaced layers in the vertical direction and three different resolutions in the horizontal (Table 2). The resolutions chosen are indicative of resolutions that could be achieved by large scale

10   Stokes simulations of ice sheets with the current generation of models. Thus they are coarser than is commonly considered to be required for self-consistent simulations involving grounding line movement (Durand et al., 2009; Pattyn et al., 2012). This is intentional, so that the current study may assess the potential for different sliding laws or basal melt parameterisations to achieve resolution-independent behaviour at coarser resolutions than is required with sliding laws similar to SR1.

The experiments are summarised in Table 3. Spin-up is performed in two stages: The first stage ("SPIN", Table 3) is from

15   a uniform thickness (300 m) slab of ice for 40 ka with paramaterised channel width 1000 km (very low buttressing). The second stage ("ADVA", Table 3) constitutes a further 40 ka with parameterised channel width 150 km (significant buttressing). This two-stage spin-up is carried out separately for each resolution and sliding law. The purpose of including buttressing is to provide a mechanism for basal melting under the shelf to impact on grounded ice. Note that basal melting is zero during the two stages of the spin-up.

20   Retreat simulations are then carried out, which form the main focus for this study. The cause of retreat is by a change in forcing, either by reducing the lateral drag back to a parameterised channel width of 150 km, or by imposing basal melting (Section 2.2) under the ice shelf, or both together. For the melt induced retreat simulations we set Ω to 0.045 or 0.009 (Table 3), resulting in typical melt rates between 1 and 10 m a^{-1}.

We also carry out re-advance experiments (ALMW and ALMN in Table 3) to test whether simulations reach the same steady

25   state in advance as in retreat under identical forcing.

Individual simulations are referred to in the results section by their "simulation code", made up of the experiment name (Table 3), the sliding relation used (Table 1) and the resolution (Table 2). For example, SPIN_SR1_R1 is the initial spin up with Weertman sliding and an element size of 3.6 km.

3   Results

30   As a "rule of thumb", we consider experiments in which the grounding line position varies across simulations of different resolution by differences of approximately the same magnitude as the size of a single element not to have significant dependency on resolution. We consider experiments with grounding line differences of several element sizes or greater to have significant

dependence on resolution. For example, differences in grounding line position of the order of 100 km between simulations at different resolutions are considered to indicate significant resolution dependency, whereas differences of the order of 1 km are not. Similarly, when we say "near to the grounding line" we are also talking in terms of element size. For example "high melt near the grounding line" can be interpreted as "high melt within a very small number of elements of the grounding line".

5   We focus mainly on the evolution of grounding line position. The spinup simulations (SPIN and ADV, Table 3) do not vary significantly with resolution, and so analysis focusses on retreat and re-advance simulations.

The spinup simulations do however vary significantly with choice of sliding relation. The steady state ADVA_SR1 profiles have their steepest surface slope close to the grounding line due to the step change in basal drag from grounded to floating ice (Figures 1 and 2). The steady state SR2 and SR4 profiles have their greatest surface slope further inland where the overburden

10   pressure becomes important. The steady state SR3 profile is similar to SR1 over most of the grounded region, but is slightly thinner due to having lower drag close to the grounding line.

Figure 2 also shows the internal shear stress in the ice for SR1 and SR3. Shear stress peaks at the grounding line for SR1 due to the step change in basal drag. The inclusion of dependence on N in SR3 leads to a gradual change, i.e. a much larger transition zone.

15   The impact of choice of sliding relation on the way the ISM responds to changing resolution is shown for retreat simulations in Figure 3. The sliding relations featuring a step change in basal drag across the grounding line (SR1, SR4a and SR4b) do not exhibit consistent behaviour with resolution, with the RBUR_SR1_R0 simulation in particular showing no retreat of the grounding line after the buttressing reduction. Note that of these simulations the magnitude of this basal drag step change is smallest for SR4b and largest for SR1. The results in Figure 3 are consistent with a smaller step change in basal drag

20   being indicative of better convergence with resolution, similar to a previous result when using a "shelfy-stream" ice sheet model (Gladstone et al., 2012). But even SR4b still shows significant resolution dependency.

The purpose of the RHMW experiment, as distinct from the RBUR experiment, is to test dependence on resolution in the presence of basal melting. Since SR1 and SR4a showed strong resolution dependence already in RBUR they have been omitted from the RHMW experiments.

25   The sliding relations in which basal drag goes smoothly to zero as the grounding line is approached (SR2 and SR3) show the most consistent behaviour with resolution in experiments RBUR and RHMW.

The SR3 simulations are unique in exhibiting an overshoot: after a strong initial grounding line retreat a small advance is seen. In the RHMW_SR3_R2 simulation damped oscillations can be seen The reason for this behaviour is not clear, but the lower resolution simulations fail to exhibit this behaviour, indicating at least some resolution dependency in this experiment.

30   In general the consistency across different resolutions appears weaker in the case of the melt-induced retreat simulations (RHMW) than the reduced buttressing simulations (RBUR).

We now look more closely at the impact of basal melting on resolution dependency. We compare retreat and advance simulations. We also investigate the impact of the water column scaling, in which zero melt is approached close to the grounding line. Sliding relation SR2 is used for these experiments as it has shown much weaker resolution dependency than SR1 and SR4,

35   and has not shown difficult-to-interpret behaviour such as the damped oscillations in RHMW_SR3_R2.

Figure 4 shows both retreat (RLMN and RLMW, red lines) and advance (ALMN and ALMW, black lines) simulations with water column scaling either on (RLMW and ALMW) or off (RLMN and ALMN). The advance simulations have identical inputs to the corresponding retreat simulations in all respects except for initial conditions. Note that while the majority of these simulations were run for 20ka, the ALMN simulations were run for 40 ka as 20 ka was not long enough to approach a steady

5   state.

In the presence of water column scaling the advance and retreat simulations approach the same grounding line position at all resolutions, showing no significant resolution dependency. This is consistent with the premise that a unique solution exists, which might be expected behaviour on a linear down sloping bed (Schoof, 2007), but has not been proven in the presence of buttressing and basal melting.

10   However, in the case where there exists a large step change in basal melt across the grounding line (ALMN and RLMN, left hand plots of Figure 4), the advance and retreat grounding lines do not approach the same final position. Behaviour is not consistent across resolutions. The fact that the advance and retreat grounding line positions are closer together at finer resolutions is consistent with the premise of uniqueness, but finer resolution simulations would be required to determine this with confidence.

15   Dependency on resolution appears to be stronger in the case of advance experiments than retreat experiments. This is in sharp contrast to the SPIN and ADVA experiments, which are a kind of advance experiment (in that the grounding line position is advancing through the simulation toward its final position), in which no significant resolution dependency was observed. This suggests that it is specifically the melting which causes resolution dependence, and that it causes greater resolution dependence in advance than in retreat.

20   The step changes in grounding line position during the early stages of retreat (Figure 4 upper panels) are typically indicative of a single element retreat for RLMW_SR2, but are typically multiple element retreat steps in RLMN_SR2.

4   Discussion

Similar to previous studies with different ice dynamic models (e.g. Pattyn et al. (2006); Durand et al. (2009); Gladstone et al. (2012)), a step change in basal drag across the grounding line also causes strongly resolution dependent behaviour in the current

25   study using the Elmer/Ice finite element Stokes flow model. A large step change causes stronger resolution dependency than a smaller step change.

A comparable resolution dependency on basal melt is shown in the current study: a step change in basal melt across the grounding line causes significant resolution dependent behaviour, worse for larger step changes.

Any resolution dependence in a model is inevitably non-physical. Ideally model behaviour should converge with finer reso-

30   lution. The experiments presented in the current study all demonstrate behaviour consistent with the hypothesis that they will converge with finer resolution. However, sufficient resolution to confirm convergence has not been achieved in some cases. More specifically experiments ALMN_SR2, RBUR_SR1, RBUR_SR4 and RHMW_SR4 failed to unambiguously demon-

strate convergence with resolution. These non-converged experiments all feature a significant step change in either basal drag or basal melt across the grounding line.

The underlying behaviour may be similar to that found by Gladstone et al. (2010a) in which a region exists containing multiple locally stable steady grounding line positions, one per grid cell or element. This region collapses to approach a single
5 point as resolution becomes finer (Gladstone et al., 2010a). If this is the case in the current study, the final positions of the advance and retreat simulations shown in Figure 4 (lower left panel) would indicate the lower and upper limits of the region.

Much weaker resolution dependence is found in the current study in the case where both basal drag and basal melt approach zero as the grounding line is approached from landward and seaward respectively. Note that the case of no basal melting is an end member example of basal melt approaching zero.
10 These results have important implications for application of model studies to real marine ice sheet systems. The presence of high basal melt rates very close to the grounding line is likely to be (at least in part) a function of the outflow of subglacial meltwater from the grounded region of the marine ice sheet. This subglacial outflow is caused by routing to the ocean of meltwater due to geothermal heating of the ice and frictional heating due to basal sliding, and can result in melt channels forming under the ice shelf (Le Brocq et al., 2013).
15 A strong subglacial outflow freshens and potentially cools the ambient ocean water in the ice shelf cavity, initiating a bouyant meltwater plume and causing significant basal melting very close to the grounding line. In the absence of strong subglacial outflow significant basal melting close to the grounding line is less likely to occur (Galton-Fenzi, 2009).

Thus marine ice sheet systems with low surface slopes near the grounding line (indicating low basal drag approaching the grounding line) and with low basal melting near the grounding line (such as might be the case in the absence of strong
20 subglacial outflow) would be achievable targets for modelling studies.

For model studies of less tractable systems, very high resolution would be needed near the grounding line, or sub-grid parameterisations (for grounding line position or cross-grounding line ice flux, for example). Parameterisations that work well for the case of no ice shelf basal melting would need to be tested in the presence of basal melting, and may need to be modified to incorporate a sub-grid treatment of basal melt.
25 The results from the current study appear to be in conflict with the findings of Gagliardini et al. (2016), who found that imposing a fixed length transition zone near the grounding line (similar to that proposed by Pattyn et al. (2006)), where the basal drag is scaled linearly to zero as the grounding line is approached (from landward), did not significantly reduce the resolution requirements. There are, however, a number of significant differences between the current study and Gagliardini et al. (2016), such as the use of a direct physical motivation to impose the drag reduction in the current study, rather than
30 imposition of linearity. We speculate that the key factor is that the imposed linear transition zone of Gagliardini et al. (2016) is typically of the same order of magnitude as the element size, meaning that the step change in basal drag across the grounding line, while moderately reduced, is not reduced by an order of magnitude or more, as in the current study for SR2 and SR3. The effect of incorporating dependence on N on the basal stress gradient approaching the grounding line is visualised for the current study in Figure 2. The transition zone is several hundred km for SR3. A future study with further simulations will be

needed to fill the gap in experiment design between the two studies to confirm whether this difference in transition zone size is the actual explanation for the differences in resolution dependence.

5 Conclusions

We have demonstrated that ISM resolution requirements for MIS simulations with an evolving grounding line are highly
5 sensitive to the physical implementation of basal sliding and ice shelf basal melting. In particular a large step change in basal drag or basal melting across the grounding line can cause strong dependence of model behaviour on resolution.

Any marine ice sheet modelling studies whose outcomes involve a moving grounding line should demonstrate convergent behaviour with resolution for parameter space relevant to their experimental setup, bearing in mind that basal drag and basal melt can both cause resolution dependence, and that resolution dependence may differ for an advancing and a retreating
10 grounding line.

We suggest that future intercomparison exercises account for a realistic sliding upstream of the GL by adopting an effective pressure dependent sliding relation and an effective pressure approaching zero at the grounding line. Instead of comparing models on a highly complicated problems requiring fine mesh resolution at the grounding line, we would then compare models on a more realistic setup, gaining in confidence in their capacity to model grounding line dynamics for real applications.

15 A significant implication is that conducting transient Stokes flow simulations of whole marine ice sheets, such as century scale simulations of the West Antarctic Ice Sheet for example, is a potentially tractable problem where evidence supports both basal drag and basal melting decreasing smoothly to zero as the grounding line is approached from respectively grounded and floating regions.

References

Asay-Davis, X. S., Cornford, S. L., Durand, G., Galton-Fenzi, B. K., Gladstone, R. M., Gudmundsson, G. H., Hattermann, T., Holland, D. M., Holland, D., Holland, P. R., Martin, D. F., Mathiot, P., Pattyn, F., and Seroussi, H.: Experimental design for three interrelated Marine Ice-Sheet and Ocean Model Intercomparison Projects, Geoscientific Model Development Discussions, 8, 9859–9924, doi:10.5194/gmdd-8-9859-2015, http://www.geosci-model-dev-discuss.net/8/9859/2015/, 2015.

Budd, W., Keage, P. L., and Blundy, N. A.: Empirical studies of ice sliding, Journal of Glaciology, 23, 157–170, 1979.

Budd, W., Jenssen, D., and Smith, I.: A 3-dimensional time-dependent model of the West Antarctic Ice-Sheet, Annals of Glaciology, 5, 29–36, 1984.

Cornford, S. L., Martin, D. F., Graves, D. T., Ranken, D. F., Le Brocq, A. M., Gladstone, R. M., Payne, A. J., Ng, E., and Lipscomb, W. H.: Adaptive mesh, finite volume modeling of marine ice sheets, Journal of Computational Physics, 232, 529–549, 2013.

Durand, G., Gagliardini, O., de Fleurian, B., Zwinger, T., and Le Meur, E.: Marine ice sheet dynamics: Hysteresis and neutral equilibrium, Journal of Geophysical Research-Earth Surface, 114, doi:10.1029/2008JF001170, 2009.

Favier, L., Gagliardini, O., Durand, G., and Zwinger, T.: A three-dimensional full Stokes model of the grounding line dynamics: effect of a pinning point beneath the ice shelf, The Cryosphere, 6, 101–112, doi:10.5194/tc-6-101-2012, http://www.the-cryosphere.net/6/101/2012/, 2012.

Favier, L., Durand, G., Cornford, S. L., Gudmundsson, G. H., Gagliardini, O., Gillet-Chaulet, F., Zwinger, T., Payne, A. J., and Le Brocq, A. M.: Retreat of Pine Island Glacier controlled by marine ice-sheet instability, Nature Climate Change, 4, 117–121, doi:10.1038/NCLIMATE2094, 2014.

Fowler, A. C.: Weertman, Lliboutry and the development of sliding theory, Journal Of Glaciology, 56, 965–972, 2010.

Gagliardini, O., Durand, G., Zwinger, T., Hindmarsh, R. C. A., and Le Meur, E.: Coupling of ice-shelf melting and buttressing is a key process in ice-sheets dynamics, Geophysical Research Letters, 37, 2010.

Gagliardini, O., Zwinger, T., Gillet-Chaulet, F., Durand, G., Favier, L., de Fleurian, B., Greve, R., Malinen, M., Martín, C., Råback, P., Ruokolainen, J., Sacchettini, M., Schäfer, M., Seddik, H., and Thies, J.: Capabilities and performance of Elmer/Ice, a new generation ice-sheet model, Geoscientific Model Development Discussions, 6, 1689–1741, doi:10.5194/gmdd-6-1689-2013, http://www.geosci-model-dev-discuss.net/6/1689/2013/, 2013.

Gagliardini, O., Brondex, J., Gillet-Chaulet, F., Tavard, L., Peyaud, V., and Durand, G.: Brief communication: Impact of mesh resolution for MISMIP and MISMIP3d experiments using Elmer/Ice, The Cryosphere, 10, 307–312, doi:10.5194/tc-10-307-2016, http://www.the-cryosphere.net/10/307/2016/, 2016.

Galton-Fenzi, B.: Modelling Ice-Shelf/Ocean Interaction, Ph.D. thesis, University of Tasmania, 2009.

Gladstone, R., Lee, V., Vieli, A., and Payne, A.: Grounding Line Migration in an Adaptive Mesh Ice Sheet Model, Journal of Geophysical Research-Earth Surface, 115, doi:10.1029/2009JF001615, 2010a.

Gladstone, R., Payne, A., and Cornford, S.: Parameterising the grounding line in flow-line ice sheet models, The Cryosphere, 4, 605–619, doi:10.5194/tc-4-605-2010, 2010b.

Gladstone, R., Payne, A. J., and Cornford, S. L.: Resolution requirements for grounding-line modelling: sensitivity to basal drag and ice-shelf buttressing, Annals Of Glaciology, 53, 97–105, doi:10.3189/2012AoG60A148, 2012.

Glen, J. W.: Experiments on the deformation of ice, Journal of Glaciology, 2, 111–114, 1952.

Gong, Y., Cornford, S. L., and Payne, A. J.: Modelling the response of the Lambert Glacier–Amery Ice Shelf system, East Antarctica, to uncertain climate forcing over the 21st and 22nd centuries, The Cryosphere, 8, 1057–1068, doi:10.5194/tc-8-1057-2014, http://www.the-cryosphere.net/8/1057/2014/, 2014.

Joughin, I., Smith, B., and Holland, D.: Sensitivity of 21st century sea level to ocean-induced thinning of Pine Island Glacier, Antarctica, Geophysical Research Letters, 37, doi:10.1029/2010GL044819, 2010.

Le Brocq, A. M., Ross, N., Griggs, J. A., Bingham, R. G., Corr, H. F. J., Ferraccioli, F., Jenkins, A., Jordan, T. A., Payne, A. J., Rippin, D. M., and Siegert, M.: Evidence from ice shelves for channelized meltwater flow beneath the Antarctic Ice Sheet, Nature Geoscience, 6, 945–948, 2013.

Leguy, G. R., Asay-Davis, X. S., and Lipscomb, W. H.: Parameterization of basal friction near grounding lines in a one-dimensional ice sheet model, The Cryosphere, 8, 1239–1259, doi:10.5194/tc-8-1239-2014, http://www.the-cryosphere.net/8/1239/2014/, 2014.

Paterson, W.: The physics of glaciers, Pergamon, Oxford, third edn., 1994.

Pattyn, F., Huyghe, A., De Brabander, S., and De Smedt, B.: Role of transition zones in marine ice sheet dynamics, Journal of Geophysical Research-Earth Surface, 111, doi:10.1029/2005JF000394, 2006.

Pattyn, F., Schoof, C., Perichon, L., Hindmarsh, R. C. A., Bueler, E., de Fleurian, B., Durand, G., Gagliardini, O., Gladstone, R., Goldberg, D., Gudmundsson, G. H., Huybrechts, P., Lee, V., Nick, F. M., Payne, A. J., Pollard, D., Rybak, O., Saito, F., and Vieli, A.: Results of the Marine Ice Sheet Model Intercomparison Project, MISMIP, Cryosphere, 6, 573–588, doi:10.5194/tc-6-573-2012, 2012.

Pollard, D. and DeConto, R. M.: Modelling West Antarctic ice sheet growth and collapse through the past five million years, Nature, 458, 329–332, doi:10.1038/nature07809, 2009.

Schoof, C.: Ice sheet grounding line dynamics: Steady states, stability, and hysteresis, Journal of Geophysical Research-Earth Surface, 112, doi:10.1029/2006JF000664, 2007.

Seroussi, H., Morlighem, M., Larour, E., Rignot, E., and Khazendar, A.: Hydrostatic grounding line parameterization in ice sheet models, The Cryosphere, 8, 2075–2087, doi:10.5194/tc-8-2075-2014, http://www.the-cryosphere.net/8/2075/2014/, 2014.

Tsai, V. C., Stewart, A. L., and Thompson, A. F.: Marine ice-sheet profiles and stability under Coulomb basal conditions, Journal of Glaciology, 61, 205–215, doi:doi:10.3189/2015JoG14J221, http://www.ingentaconnect.com/content/igsoc/jog/2015/00000061/00000226/art00001, 2015.

Vieli, A. and Payne, A.: Assessing the ability of numerical ice sheet models to simulate grounding line migration, Journal of Geophysical Research-Earth Surface, 110, doi:10.1029/2004JF000202, 2005.

Weertman, J.: On the sliding of glaciers, J. Glaciol., 3, 33–38, 1957.

Table 1. Sliding relations and constants used in the current study.

Sliding Relation	Equation	C	z_o
SR1	3	10^{-3} MPa m$^{-\frac{1}{3}}$ a$^{\frac{1}{3}}$	-
SR2	4	7×10^{-6} MPa m$^{-\frac{4}{3}}$ a$^{\frac{1}{3}}$	-
SR3	5	10^{-3} MPa m$^{-\frac{1}{3}}$ a$^{\frac{1}{3}}$	-
SR4a	6	4×10^{-6} MPa m$^{-\frac{4}{3}}$ a$^{\frac{1}{3}}$	100 m
SR4b	6	4×10^{-6} MPa m$^{-\frac{4}{3}}$ a$^{\frac{1}{3}}$	50 m

Table 2. Model resolutions used in the current study.

Resolution	Number of elements in the horizontal	Element size in the horizontal
R0	250	7.2 km
R1	500	3.6 km
R2	1000	1.8 km

The Cryosphere

Discussions

Open Access

EGU

Table 3. Summary of experiments. The experiment name is given in bold for experiments whose results are analysed in the current study. Experiments not given in bold provide spinup/initialisation for those analysed. The basal melt forcing is described in Section 2.2 and the experimental design in Section 2.3. W is parameterised channel width, S_w is the water column thickness scaling of basal melt (equation 8), and Ω is a basal melt tuning parameter.

Experiment	Description	Initial condition	W	S_w used?	Ω
SPIN	Initial spin up	Uniform slab ($H = 300$m)	1000 km	-	-
ADVA	Advance due to buttressing increase	SPIN final state	150 km	-	-
RBUR	Retreat due to buttressing reduction	ADVA final state	1000 km	-	-
RHMW	Retreat due to high basal melt (with water column scaling)	ADVA final state	150 km	Yes	0.045
RHBW	Retreat due to high basal melt (with water column scaling) and buttressing reduction	ADVA final state	1000 km	Yes	0.045
RLMW	Retreat due to low basal melt (with water column scaling)	ADVA final state	150 km	Yes	0.009
ALMW	Advance due to lowering of basal melt (with water column scaling)	RHBW final state	150 km	Yes	0.009
RHBN	Retreat due to high basal melt (no water column scaling) and buttressing reduction	ADVA final state	1000 km	No	0.045
RLMN	Retreat due to low basal melt (no water column scaling)	ADVA final state	150 km	No	0.009
ALMN	Advance due to lowering of basal melt (no water column scaling)	RHBN final state	150 km	No	0.009

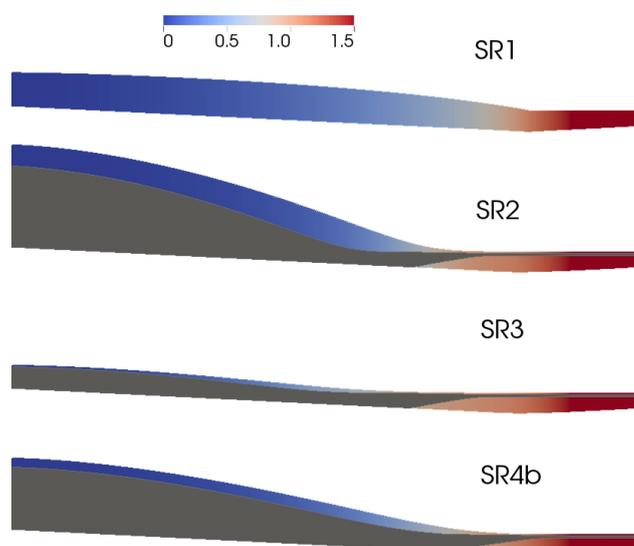The Cryosphere

Open Access

Discussions

EGU

Figure 1. Vertically exaggerated (100 times) steady state profiles from the ADVA experiment. Resolution R2 is shown, but these profiles do not vary significantly with resolution. The colour scale shows ice velocity in km a^{-1}. These profiles provide the starting point for the retreat simulations. The final state of the melt-induced experiment RHMW is overlain in grey (note that there is very little vertical shear in the velocity profiles).
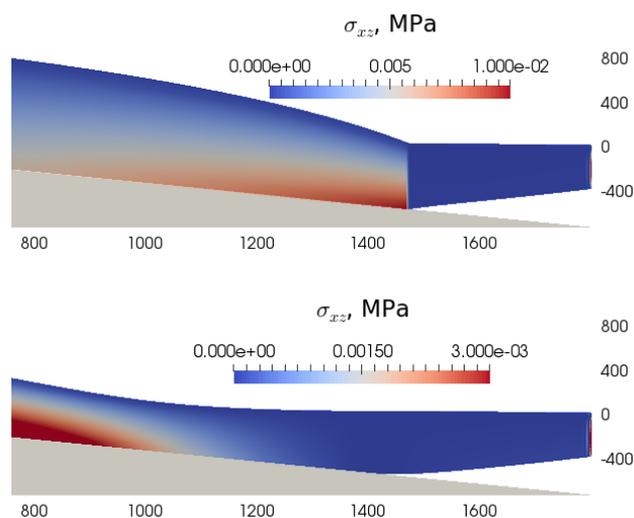
Figure 2. Stress tensor component σ_{xz} (internal shear stress) shown at the end of the ADVA experiment for SR1 (top) and SR3 (bottom) for the seaward 1000 km of the domain. Note the different colour scales. Distance from the ice divide is shown along the bottom in km. Height relative to sea level is shown at the right end of the plots in m. Bedrock is shaded in grey. Vertical exaggeration is 200 times.
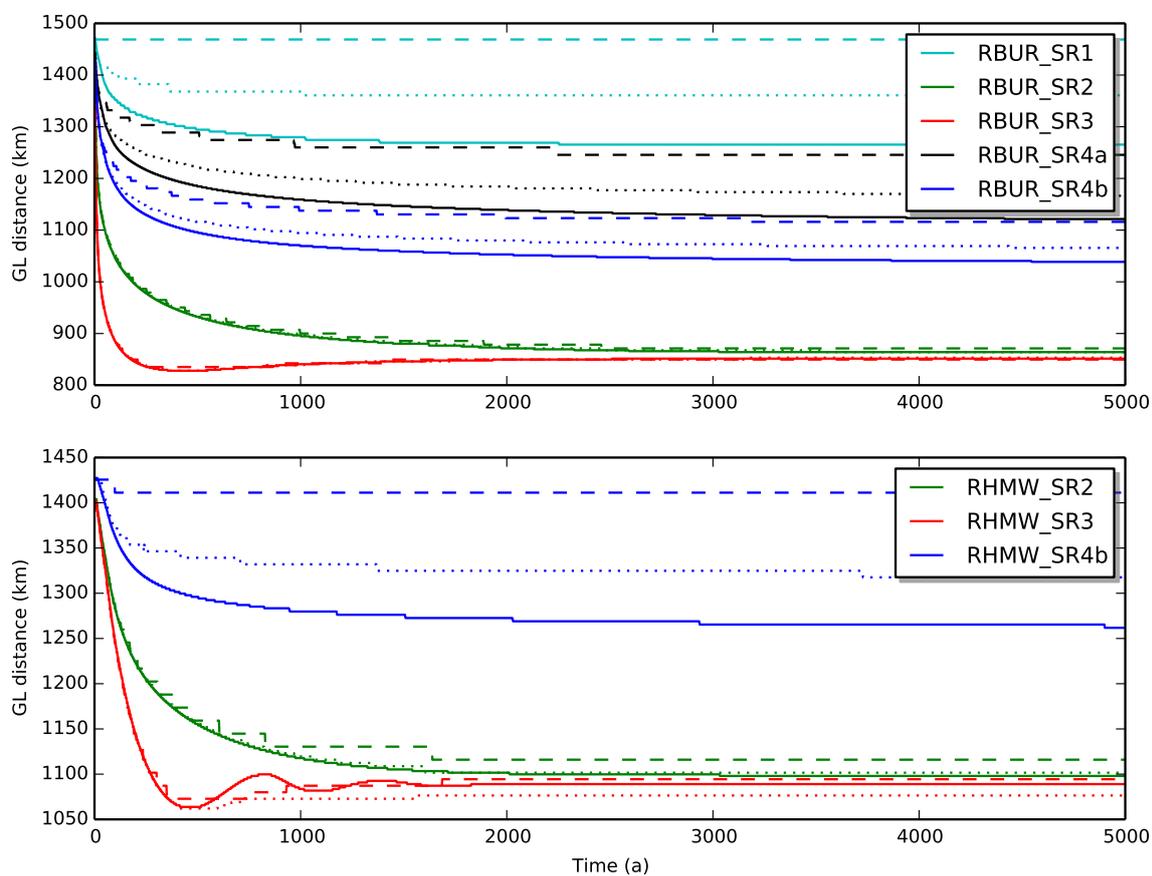
The Cryosphere
Discussions

Open Access

EGU

Figure 3. Evolution of grounding line position during retreat simulations with different sliding relations. Sliding relations are described in Section 2.1 and Table 1. Experiments are described in Section 2.3 and Table 3. Resolutions (Table 2) are coarse (R0, dashed line), medium (R1, dotted line) and fine (R2, solid line).
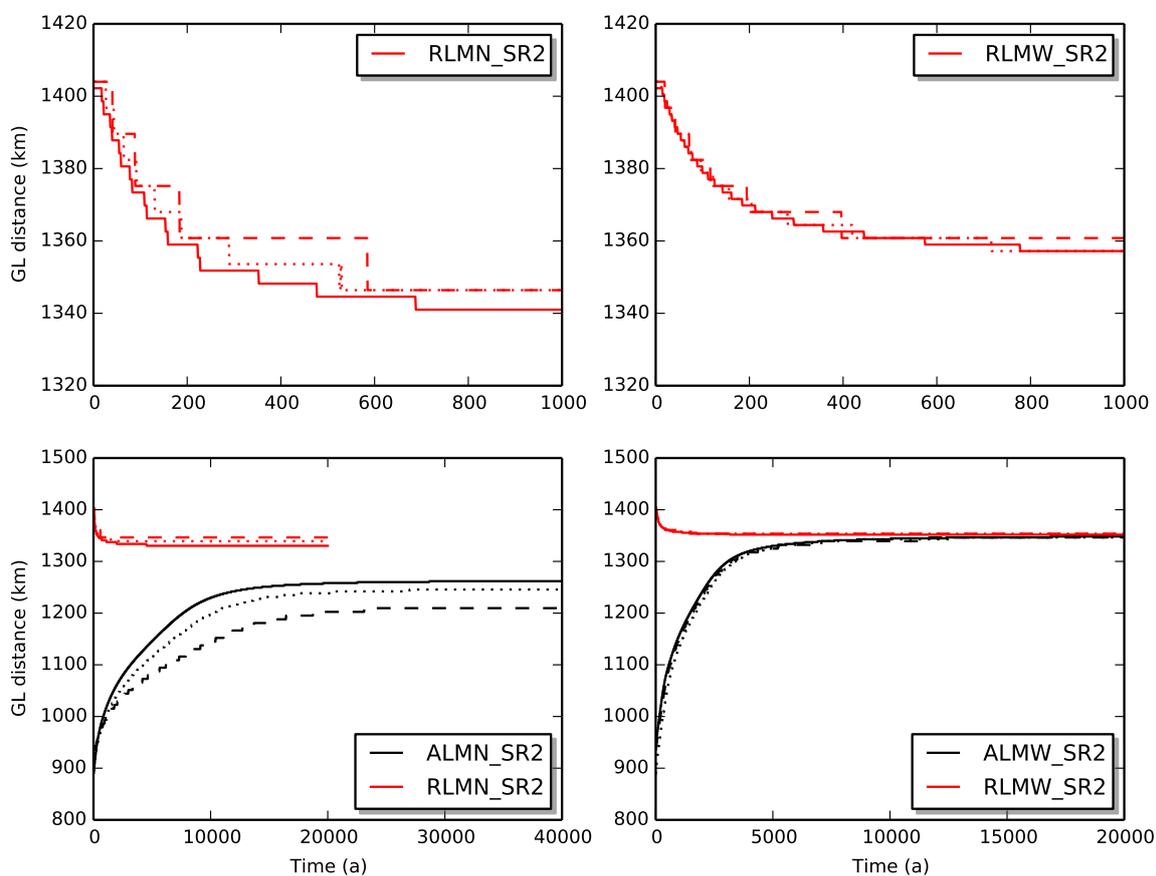
The Cryosphere
Discussions

Open Access

EGU

Figure 4. Evolution of grounding line position during the sub-shelf melting simulations with effective pressure dependency in the basal sliding relation. The upper panels show the detail of the early stages of the simulations, whereas the lower panels show the full simulations. The sliding relation (SR2) is described in Section 2.1 and Table 1. Experiments are described in Section 2.3 and Table 3. Resolutions (Table 2) are coarse (R0, dashed line), medium (R1, dotted line) and fine (R2, solid line).